

Chapter-2

Instrumentation and Techniques

This chapter describes briefly 15UD Pelletron Accelerator and the techniques used for characterization of the samples i.e. FTIR Spectroscopy, LCR Meter, Optical Microscopy, SEM, Vickers' Microhardness, and Instron Tensile Tester.

Chapter 2

Instrumentation and Techniques

2.1	Introduction	71
2.2	Pelletron Accelerator	72
2.2.1	The Injector System	75
2.2.2	Source of Negative Ions by Cesium Sputtering (SNICS).	76
2.2.3	Main Accelerator Column.	77
2.2.4	Analyzer Magnet.	79
2.2.5	Vacuum System.	80
2.2.6	The Charging System.	80
2.2.7	The Control System.	80
2.2.8	High Energy Beam Lines.	81
2.2.9	Material Science "UHV" Beam Line.	81
2.3	Characterization Techniques of Irradiated Polymers.	82
2.3.1	AC Electrical Properties.	83
2.3.1(a)	Dielectric in the Electric field.	85
2.3.1(b)	Conduction in Dielectric.	85
2.3.1(c)	Conductivity and Resistivity.	86
2.3.1(d)	Dielectric loss and Capacitance.	88
2.3.2	Fourier Transform Infra Red Spectroscopy.	91
2.3.3	Optical Microscopy	95
2.3.4	Scanning Electron Microscopy.	97
2.3.5	Vickers' Microhardness Indenter.	99
2.3.6	Instron Tensile Tester.	101
2.3.7	Thermogravimetry Analysis.	106
	REFERENCES.	110

Chapter 2

Instrumentation and Techniques

2.1 Introduction

This chapter deals with a brief description of the equipments with their relevant details and specifications used in the experiments carried out and various techniques for the off-line measurements employed in this thesis. The present experimental work involves the following stages

1. Irradiation of polymers using 15UD Pelletron accelerator at NSC, New Delhi. A brief description about the instrument is described in this chapter.
2. The characterization techniques that are commonly used for the off-line measurements to study electrical, thermal, structural and mechanical properties of the pristine and irradiated samples are discussed. Electrical (viz. Resistance, capacitance and $\tan \delta$ measurement) using an LCR meter, Thermal Stability by TGA, Structural Analysis by FTIR Spectroscopy, Surface Morphology by Optical Microscope / SEM, Hardness measurement by Vicker's Microhardness Indenter and Tensile Strength (i.e. Breaking load, Elongation and Yield point) by Instron Tensile Tester.

In the following sections, the important aspects of instruments used and various experimental techniques employed are presented.

2.2 Pelletron Accelerator

The 15 UD Pelletron accelerator at the Nuclear Science Center (NSC) [1] belongs to a class of particle accelerators known as Van de Graff electrostatic accelerator. It is capable of accelerating almost any ion beam from Hydrogen to Uranium. The energy of the beam can be from a few MeV (million electron volts) to hundreds of MeV. A schematic diagram showing the basic principle of accelerator is shown in the **Figure 2.1**. In this machine, negative ions are produced and pre-accelerated to ~ 400 KeV, the mass is analyzed and then injected into a strong electrical field inside the accelerator. At the center of the accelerator tank there is a terminal shell, which is maintained at high voltage (up to 15 million volts). The negative ions on traveling through the accelerating tube from the top of the tank to the positive terminal get accelerated. On reaching the terminal, they pass through a stripper that strips the ions off their electrons, thus transforming them to positive ions. These positive ions are repelled from the terminal (due to positive potential) and thus are again accelerated to ground potential to the bottom of the accelerator, the same terminal potential is used twice to accelerate the ions. On exiting from the accelerator, the ion beam corresponding to a particular energy (selected) is bent by an analyzing magnet. The switching magnet diverts the high-energy ion beam to the desired experimental station. A schematic diagram of the accelerator facilities at NSC is shown in the **Figure 2.2**. A brief description of the important parts of the accelerator is also given below.

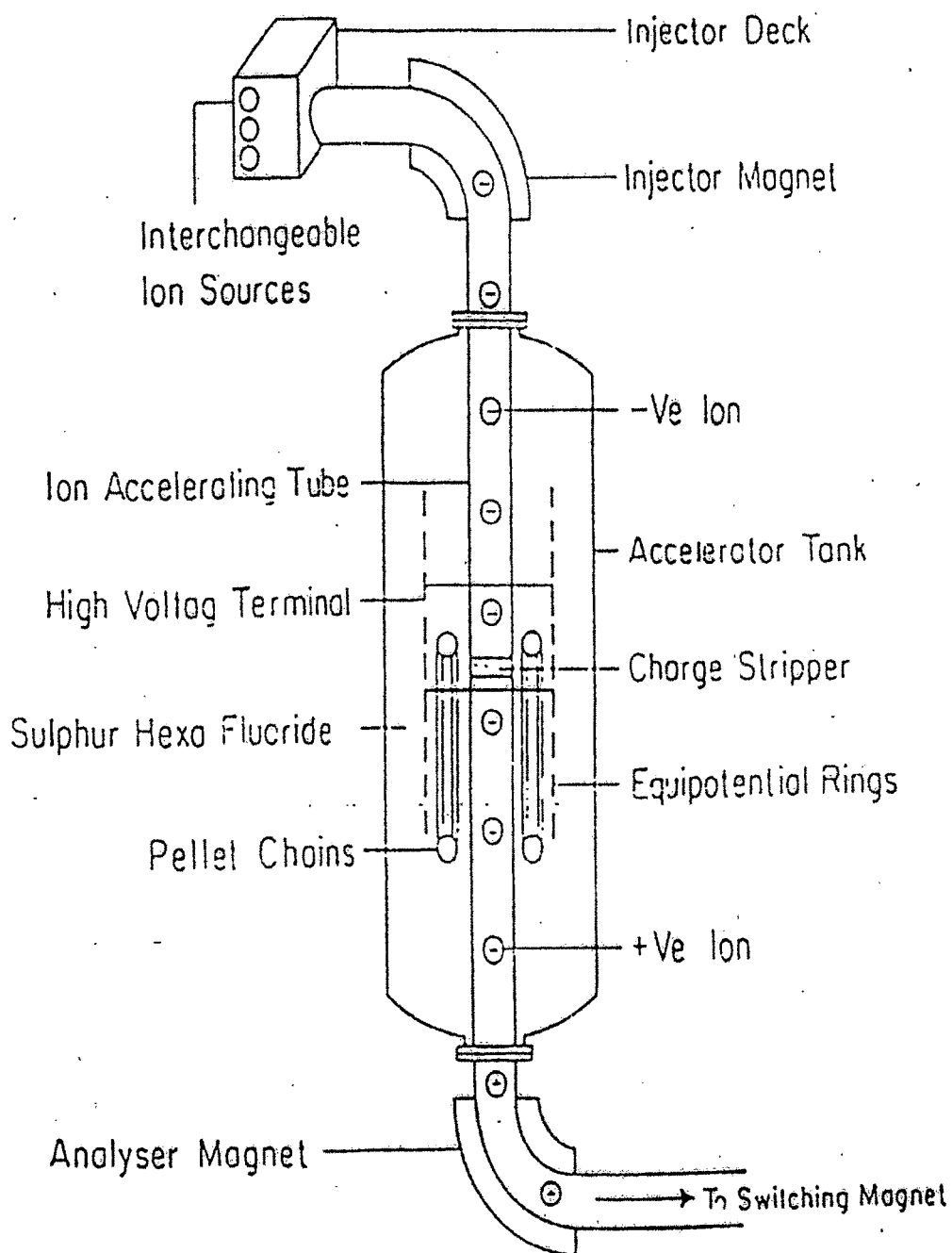


Figure-2.1 A Schematic diagram showing the basic principle of acceleration in Pelletron.

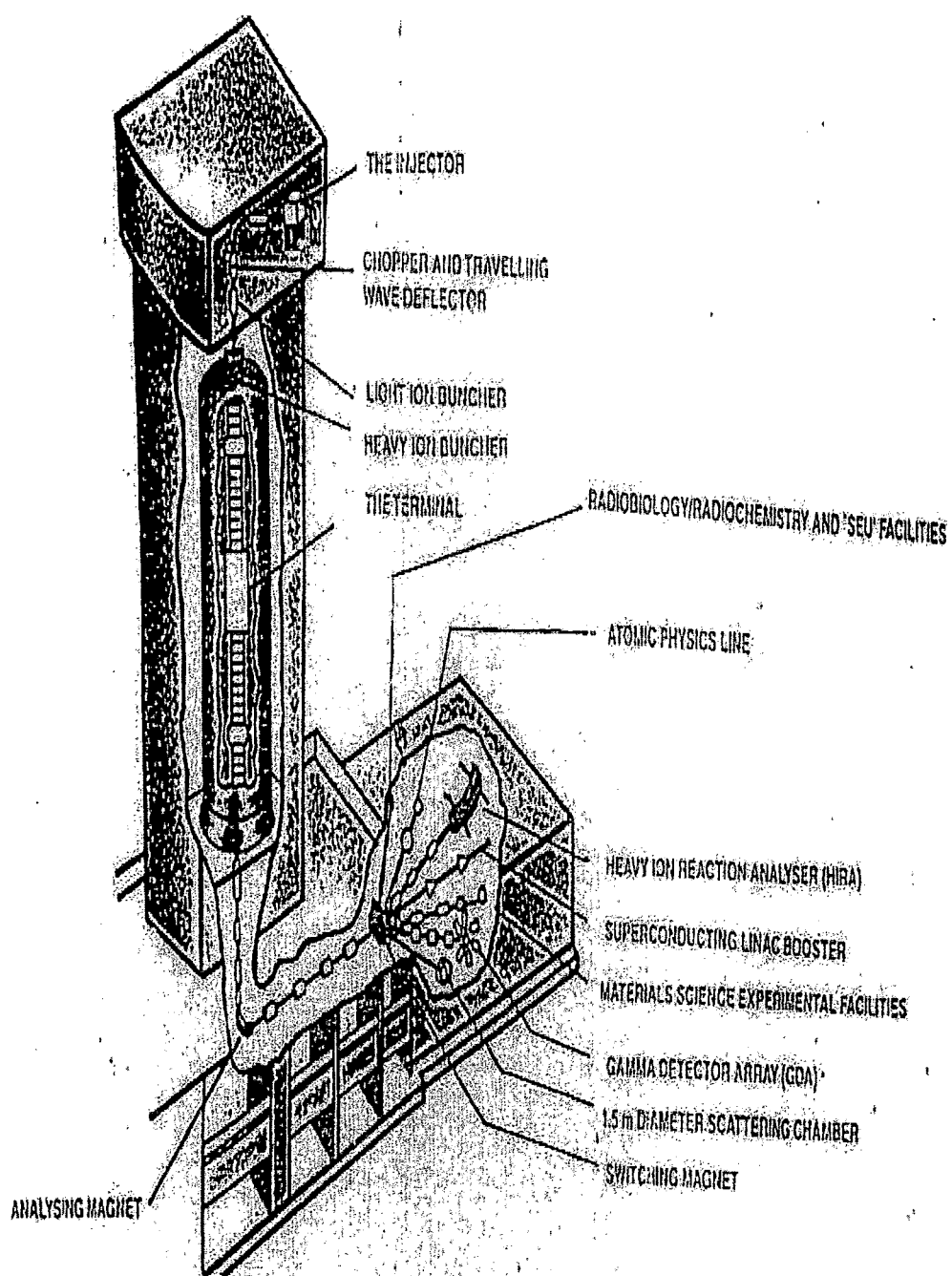


Figure-2.2 A Schematic diagram of the accelerator facilities at NSC

2.2.1 The Injector System

This system consists of mainly, an ion source, a pre-accelerator tube and the bending magnet injector. The ion sources are mounted inside an isolated, cubical rack called the ion injector deck. Three negative ion sources, have been provided:

- 1) Source of negative ions by cesium sputtering (SNICS) which can produce negative ions of almost all elements (noble gases are exceptions).
- 2) Radio frequency (R.F.) gas ion source (alphatross) mainly used for He⁻ ions.
- 3) Direct extraction negative ion (Duoplasmatron) mainly used for H⁻ ions.

For our experiment SNICS ion source was used. The operation and design of this ion source will be discussed in more detail in the next section. The negative ions produced by any one of these ion sources housed in a high voltage deck biased to a negative potential (-400 KV with respect to ground) pre-accelerates the ions produced in the source traveling to the ground. Initially by adjusting the extractor and focus voltages the beam is focused onto the double slit in the object plane of the injector magnet. The position and size of the beam is continuously monitored at beam profile monitor (BPM) before the double slit. The beam is centrally aligned by means of electrostatic steerer before the BPM. Then the Faraday cup (FC) housed after the double slit measures the beam current. The magnetic field in the injector magnet is adjusted so that singly charged ion beam of a particular mass can pass through the magnet and get focused on the double slit, on the image plane of the magnet. The position and focusing of the beam selected by the magnet is monitored by another BPM and the current is measured

by FC following it. Afterwards two sets of electrostatic quadrupole are used to focus the beam at the entrance of the accelerating columns.

2.2.2 Source of Negative ions by cesium sputtering (SNICS)

Most tandem accelerators use high intensity cesium sputter ion source such as sources of Negative ions by Cesium Sputtering (SNICS) due to the fact that they are versatile, easy to operate and provide negative ions of almost all elements (noble gases like He, Ne, Ar etc being the exceptions). The principle of operation of such a source is as follows- A primary Cs^+ ion beam is produced by surface ionization of Cesium vapour on a high work function, high melting point metallic surface (such as tantalum) maintained at a temperature of about 1100°C . This primary beam is then focused onto the source material by suitable electric field configuration. The cathode, which is placed at a negative potential of a few kilovolts, contains the material of which the ions are to be produced. The primary Cs^+ beam gets accelerated towards the cathode and sputters the source material to form negative ions, which are extracted by means of suitable potentials. As the Cs^+ ions hit the cathode, it becomes hot and hence freon cooling is used to cool the cathode.

Figure 2.3 shows a schematic diagram of SNICS multi-cathode ion source used on the injector of the NSC Pelletron accelerator. In this ion source, a spherical geometry ionizes to improve the cesium ion focusing, an immersion lens in the form of a circular plate with a central aperture to focus the negative ion beam and a wheel capable of holding up to 24 source materials with a simple rotation mechanism are used.

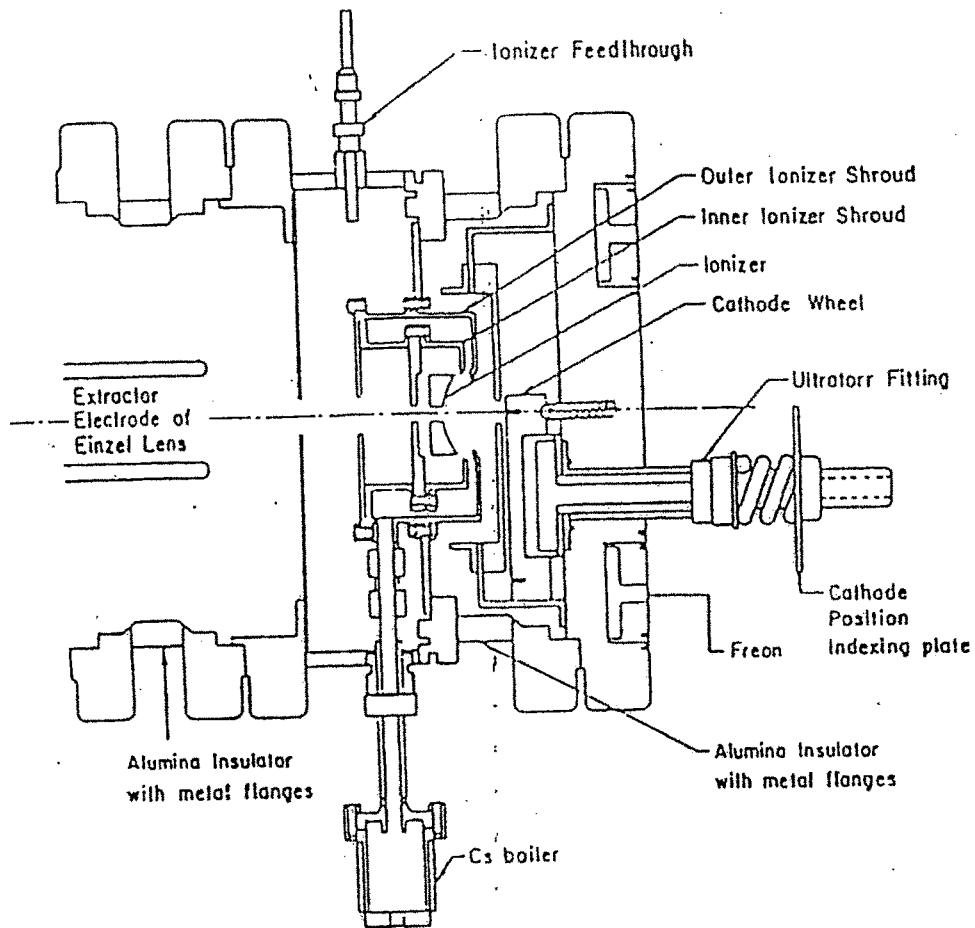


Figure - 2.3 Schematic diagram of the NSC multi-cathode ion source.

2.2.3 Main Accelerator Column

The Pelletron Accelerator Column is a vertical configuration installed in a steel tank, which is 26.5 meter long and 5.5 m in diameter and filled up with Sulphur Hexafluoride (SF_6) gas at a pressure of about 6-7 bar. The SF_6 gas is used because of the following advantages. It is inflammable, non-toxic, has excellent heat transfer property, high recombination rate and high dielectric strength (three times greater than

N₂). The high voltage terminal of about 1.52 m in diameter and 3.81 m in height is located inside the tank. The terminal can be charged to a high potential (4MV-15MV) and is connected to the tank vertically through ceramic-titanium tubes called accelerating tubes. A potential gradient is maintained through these tubes by a total of thirty units of ~1MV potential each by placing 15 such units on each side of the terminal. The upper portion (above the terminal) of the column is referred to as the low energy section while the portion below is called the high-energy section. Two shorted units with no potential gradient commonly known as dead sections, are also provided, one each in the low and high energy column sections for housing the vacuum pumps and other beam handling equipment. Both sections are provided with an electron trap and a sputter ion pump. The low energy dead section is also provided with an electrostatic quadrupole triplet lens while the high-energy dead section is equipped with a second foil stripper assembly.

Negative ions injected into the accelerator column are accelerated to the terminal. The terminal has a foil stripper assembly (thin carbon foil) as well as a gas stripper (nitrogen gas at low pressure). As the ions pass through the stripper, it strips off some of the electrons to become positive ions. Depending on the foil thickness (or gas pressure), the incident energy and type of the ions, the charge state distribution of the emerging positive ions will vary. The most probable charge state and the other charge states after stripping can be calculated by semi-empirical formulae. These ions are further accelerated while traveling to the high-energy end of the accelerator. As a result the ions emerging out of the accelerator column gain energy given by:

$$E_i = [E_{inj} + (1+q_i) V] \text{ MeV}$$

Where, E_i = energy of the ion having charge state q_i after stripping.

V = Terminal potential in MV (million volts)

E_{inj} = Energy of the injected particle in MV.

The ion beam emerging from the accelerator is focused at the object point of the analyzing magnet by means of magnetic quadrupole triplet lens placed at the accelerator exit.

2.2.4 Analyzer Magnet

As it has been discussed earlier, the Pelletron ion beam is generally, composed of several components, each with different charge state and energy. However for the experimental purpose, precise monoenergetic ions are required. So the Pelletron high energy beam line following the main accelerating tube includes an energy dispersive, homogeneous dipole magnet, which can be set such that all unwanted ion beam components are filtered out leaving only the selected components for onward transmission to the beam lines. For an ion beam having mass M , energy E and charge state q , the analyzing field required for selection of such a beam is governed by the relation

$$B = K (ME)^{1/2} / q$$

Where, K is a constant. Setting different magnetic field strengths (B) one can choose different values of M , E and q of the ions.

2.2.5 Vacuum System

The entire beam transport system of the 15UD Pelletron accelerator is maintained under a clean ultra high vacuum condition i.e. at pressure below 1×10^{-9} Torr. This is achieved by the use of different types of vacuum pumps distributed all along the beam line from the ion source to the irradiation chamber.

2.2.6 The Charging System

The Pelletron terminal is charged to its high voltage using two charging chains inside the accelerator. The chains consist of small stainless steel cylinders joined together by small nylon insulating links to form a single, long, endless chain. These cylinders are called pellets. The process of charging is done by induction. The charger is induced on the pellets of the chain by a cylindrical plate called inductor, which is connected to a – 50kV power supply. The chain moves on two pulleys driven by a motor at high speed, carrying the charge Q to the terminal. The terminal is charged to a voltage V where Q/V is the Capacitance C between the terminal and the accelerator tank.

2.2.7 The Control System

The accelerator is controlled from a control room through a PC-AT 386 computer with EGA graphics card, MS-DOS operating system and suitable control software. The devices to be controlled at various locations of the accelerator are connected to the computer Automated Measurements and Control (CAMAC) crates. The signals from the computer through the main CAMAC crate situated in the control room to the crates,

placed at other locations and vice-versa are sent through a CAMAC serial highway. The devices located at high potentials are connected to the CAMAC crate by using fiber optics cables. The software, written entirely in C language, is database oriented and is modular in nature. The entire set-up can be saved in a data file for a future run. A separate relay driven safety interlock monitor is provided to display the door interlocks and radiation levels at various locations.

2.2.8 High Energy Beam Lines

The ion beam of a desired energy (E) and mass (M) is transported into any one of the seven beam lines of the beam hall by means of a switching magnet. The beam is kept centered and focused by means of a steering and magnet. The beam is visually monitored by beam profile monitors and the beam current is measured by means of Faraday cups.

2.2.9 Material Science 'UHV' Beam line

One of the beam lines of the Pelletron is terminated into material science ultra high vacuum (UHV) chamber line. This beam line is situated at +15°C, where the magnetic rigidity of the switching magnet is high. The vacuum attainable in the UHV chamber (volume ~150 lt) is below 10^{-3} Torr by the pumping combination of an Ion pump (400 lt/sec.), a 'Titanium Sublimation Pump (TSP) and a 'Turbo' molecular pump (250lt/sec.). To study on-line radiolysis processes in ion irradiated polymers, a Quadrupole Mass Spectrometer (QMS) was installed in the UHV chamber prior to the present irradiation work. Also a 'UHV' target ladder, heaving the in-vacuum sample

transfer facility was incorporated in the irradiation chamber, for our irradiation work. To accurately measure the integrated number of impinging ions on the samples, we connected current integrator with one of the UHV electrical feed through. ACCTV Camera was also attached to one of the ports of chamber for viewing the sample position.

2.3 Characterization Techniques for the Analysis of Irradiated Polymers.

The bombardment of materials with energetic ions or atoms can give rise to many changes within the target material. These changes may be due to damage of the target caused by the transfer of energy from the incident particles to the atoms of the target or they may be due to the chemical effects of the incident particles once they have come to rest in the target or a combination of both. In order to understand the interaction of the incident particles with the target material, it is necessary to measure the changes that have been induced in the target due to exposure to the incident beam of ions or atoms.

The modification of the properties of materials by ion bombardment has been the subject of intensive research in many laboratories since the late 1960's. In fact, it has been the possibility that ion bombardment may improve certain properties of materials that have been the driving force behind much of this research. In large part, the early work was purely phenomenological, relating an observed change in macroscopic properties such as hardness or chemical reactivity to the implanted ion species or dose.

However, these changes in macroscopic properties are due to alterations in microstructural properties such as chemical bonding and phase distribution. In order to develop an understanding of why the macroscopic changes occur and how to optimize the changes for a particular application, it is necessary to characterize the microstructure of ion bombarded materials and relate the alterations in microstructure caused by the bombardment to the macroscopic changes.

Most ion implantation research has been carried out on metals or semiconductor targets with much less attention being paid to implanted insulators and thus most of the characterization methods that have been developed, have been applied primarily to metals and semiconductors. Some of these methods are also useful for ion bombarded insulators [2].

2.3.1 AC Electrical Properties

Many polymeric materials have been very successful in electrical applications because of one or more outstanding properties, such as dielectric strength, volume and surface resistivity, dielectric constant, loss factor and dissipation factor. Electrical properties are not a function of molecular weight in high polymers. Crystallinity can affect the dielectric constant. Electrical properties are influenced more by dipole asymmetry than by the presence of polar groups. Polytetra fluoroethylene, for example has a lower dissipation factor than Poly Vinyl Floride; the latter possesses a greater dipole asymmetry than the former.

When the dipoles are able to respond readily to change in the electric field (low frequency or high temperature) the dielectric constant is high. At high and low frequencies, the dipoles can either respond completely or not at all to the change in field, and the loss factor which is the product of dielectric constant and power factor is low. The power factor is the sine of the angle of phase difference due to the delay in movement of the dipole with the change in the field.

Although the various types of radiation interact with matter in different ways, the primary process is the production of ions and electrically excited states of molecules which in turn, may lead to the formulation of free radicals, radiation generated mobile electrons, which become trapped at sites of low potential energy. The first phenomenon leads to permanent chemical, mechanical and electrical changes of the materials, while the second results in temporary electrical changes in performance [3].

In polymeric materials, the formation of the free radicals during irradiation leads to scission and cross-linking process that modify the chemical structure of the insulation, generally leading to deterioration of the mechanical properties. This mechanical deterioration frequently gives rise to significant electrical property changes. However, important electrical property changes sometimes occur before mechanical degradation. The extent of scission and cross-linking processes depends on the absorbed dose, the absorbed dose rate, the material geometry and the environmental conditions present during the irradiation. Because the free radicals some times decay slowly, there may also be post irradiation effects.

2.3.1 (a) Dielectric in the Electric field.

The main process that takes place in any dielectric under the influence of the electric field is polarization, i.e. limited displacement of bound charges or orientation of dipole molecules. The phenomenon underlying dielectric polarization may be judged from the permittivity (dielectric constant) and the dissipation factor (loss angle or loss tangent), if the polarization of the dielectric is attended by the thermal dissipation of electrical energy, which heats the dielectric.

Heating of a commercial dielectric may result from free charges present in small amount in its body, which causes the flow of a small leakage current (conduction current) under the effect of the applied voltage. The presence of this current in the dielectric body and over its surface attests to electrical conduction in the dielectric, which can quantitatively be expressed in terms of the volume and surface conductivities, respectively, being inversely proportional to the volume and surface resistivities[4].

2.3.1 (b) Conduction in dielectrics.

The process of displacement of bound charges, which proceeds in a substance until equilibrium is reached, gives rise to polarization or displacement currents in the dielectrics. When an electronic or an ionic polarization takes place, the displacement currents of the elastically bound charges last for so short a time that the measuring instruments fail to register them. The displacement currents attributed to various slow-

acting (relaxation) mechanism of polarization are called absorption currents, which appear in most commercial dielectrics. When a dielectric is placed in a d.c. field, the absorption currents flows in opposite directions only at moments when the circuit is closed or opened; with the alternating voltage in a circuit the displacement currents persist for so long, as the dielectric remains in the electric field. The presence of a small number of free charges in commercial dielectric results in small leakage or conduction currents. Thus, the total density of currents in a dielectric is the sum of the leakage current density and the displacement current density.

$$J = J_l + J_{ab} \quad (2.1)$$

The displacement current density depends on the rate of change of vector \vec{D} (the electric flux density or dielectric displacement).

$$J_{ab} = \frac{d\vec{D}}{dt} \quad (2.2)$$

The rate of change of \vec{D} being governed by the types of charge displacement, i.e. by polarization mechanisms (ionic, electronic and slow acting) [5].

2.3.1 (c) Conductivity and Resistivity.

Most polymers are good insulators in their unfilled state with materials such as polyethylene, polytetrafluoroethylene and polystyrene being among the best insulators known. The conductivity of a material is given by the basic equation

$$\sigma = qn\mu \quad (2.3)$$

Where q is the charge on the carrier, n is the concentration of carriers and μ is the drift mobility of the carriers. n and μ are determined by molecular structure and depend on factors such as temperature and applied field.

Conduction may be either electronic with electrons and holes as carriers, or ionic with cations and anion as carriers. In most polymeric materials, it is difficult to detect any electronic conductivity and most of the conductivity that is observed is due to impurity ions such as catalyst residues, dissociable end groups and degradation products. Therefore, the resistivity ρ (reciprocal of conductivity) of a polymeric material may be significantly improved by purification of the polymer. Polyamides, however, do display pronounced ionic conduction at elevated temperatures which increase by several orders of magnitude between ambient temperature and 100°C. This is probably due to the dissociation of amide groups to give protons with mobility possibly aided by the hydrogen bonding network. Inherently conductive polymers such as polyacetylene and polypyrrole are now more widely researched and some commercial applications are being considered. Polymers that are rendered conducting by the incorporation of carbon black or metal particles are widely used [6].

The volume resistivity, ρ_v , of a material is the resistance between opposite faces of a unit cube and is an important material parameter in polymer insulation. The surface resistivity, ρ_s , (the resistance between opposite edges of a unit square), may also be of importance. For high resistivity materials, ρ_v may be measured as a rectangular or

cylindrical block of material with electrodes attached to the ends. The volume resistivity, ρ_v , is then given by

$$\rho_v = \frac{RA}{T} \quad (2.4)$$

where R is the measured resistance, A is the cross-sectional area of the electrode and T is the specimen thickness. For low resistivity materials, ρ_v , is best measured on a thin disc of polymer with electrodes painted on either side.

The conductivity is calculated as $1 / \rho_v$ i.e.

$$\begin{aligned} \sigma_v &= 1 / \rho_v \\ \sigma_v &= T/RA \end{aligned} \quad (2.5)$$

The surface resistivity, ρ_s , may be measured using concentric ring electrodes. ρ_s is given by

$$\rho_s = 2\pi R \ln(r_1/r_2) \quad (2.6)$$

Where r_1 and r_2 are the radii of inner and outer electrodes, respectively.

2.3.1 (d) Dielectric loss and Capacitance

The dielectric loss in an insulating material can be described by the power dissipated per unit volume, called the specific loss; often, in evaluating the degree to which a dielectric can dissipate the energy of the field, use is made of the angle of dielectric loss and also the tangent of this angle. The dielectric loss angle δ is the complement of the dielectric phase angle ϕ to 90° . The angle ϕ is the angular difference in phase between

the voltage and current in the capacitive circuit. In the ideal case, the current phasor in such a circuit will lead the voltage phasor by 90° , and the loss angle δ will be zero. As the thermal dissipation of the electrical energy rises, the phase angle φ decreases, but the dielectric loss angle grows and so does its function $\tan \delta$ [7].

It is possible to distinguish four major types of dielectric loss according to their nature and characteristic features.

- (1) dielectric loss due to polarization
- (2) dielectric loss due to leakage current
- (3) dielectric loss due to ionization
- (4) dielectric loss due to structure heterogeneity.

Along with the dielectric losses due to leakage-current conduction and slow acting polarization, other types of losses occur in dielectrics, which heavily affect their electrical properties. These losses result from conducting or semiconducting foreign inclusions of carbon, iron oxides etc. Even a small content of these impurities causes high power loss [8].

Consider a parallel plate capacitor in vacuum. The charge per unit area $+Q$ and $-Q$ stored in the plates are directly proportional to the field.

$$Q = \epsilon_0 E \quad (2.7)$$

Where E is the electric field and ϵ_0 is the permittivity of free space. The vacuum capacitance per unit area of electrode C_0 is defined as

$$C_0 = \frac{Q}{V} \quad (2.8)$$

Where V is the applied voltage.

When a dielectric is introduced between the plates of a capacitor, it becomes polarized and at low fields the polarization is proportional to the field. As a result of polarization, more charge is stored on the capacitor electrodes for the same applied voltage as in vacuum, thereby increasing the capacitance of the system. The ratio of the increased (measured) capacitance to the vacuum capacitance is ϵ , the relative permittivity (i.e. dielectric constant), is given by

$$\epsilon = \frac{C}{C_0} \quad (2.9)$$

$$C_0 = \frac{\epsilon_0 A}{T}$$

Where C is the measured capacitance and

ϵ_0 is the permittivity of free space (8.854×10^{-12} F/m)

A is area of the electrode and

T is the thickness of the sample.

In an alternating field, there will be two components as a result of polarization alternating in direction, (1) leading to dipolar orientation and (2) lagging behind the applied field. The complex dielectric constant ϵ^* is given by

$$\epsilon^* = \epsilon' - i\epsilon'' \quad (2.10)$$

where ϵ' relates to the energy stored in a cycle and ϵ'' relates to the energy lost or dissipated per cycle and is known as the dielectric loss factor.

Tan δ , the dielectric loss tangent or dissipation factor, is defined as

$$\tan \delta = \epsilon'' / \epsilon' \quad (2.11(a))$$

$$\tan \delta = \frac{\text{energy lost or dissipated per cycle}}{\text{energy stored}} \quad (2.11(b))$$

A whole range of techniques are available for measuring dielectric properties such as the loss factor ($\tan \delta$), and dielectric constant and the technique employed depend to some extent on the frequency range. At low frequencies, up to around 10^6 Hz, bridge techniques can be used. These are the most common methods for determining dielectric properties. The equivalent electrical circuit for a sample is determined at a given frequency by balancing the bridge circuit [9].

In the present study we have used variable frequency LCR meter (General Radio, USA, model 1689) in the frequency range 0.05 to 100KHz, at ERDA, Baroda.

2.3.2 Fourier Transform Infra Red Spectroscopy

The term infrared spectroscopy normally is used to connote the measurement of the absorption of radiation as a function of wavelength in the “analytically useful” portion of the infrared spectrum [10]. Most common infrared spectrometers operate between wavelengths of 2.5 to 25 or 50 micrometers. As an alternative to wavelength, wavenumbers are used, which are proportional to frequency or energy and are simply equal to the reciprocal of the wavelength, usually given in cm^{-1} (1 wavenumber = 1 cm^{-1})

An infrared absorption experiment can be visualized with reference to the **Figures 2.4 and 2.5**

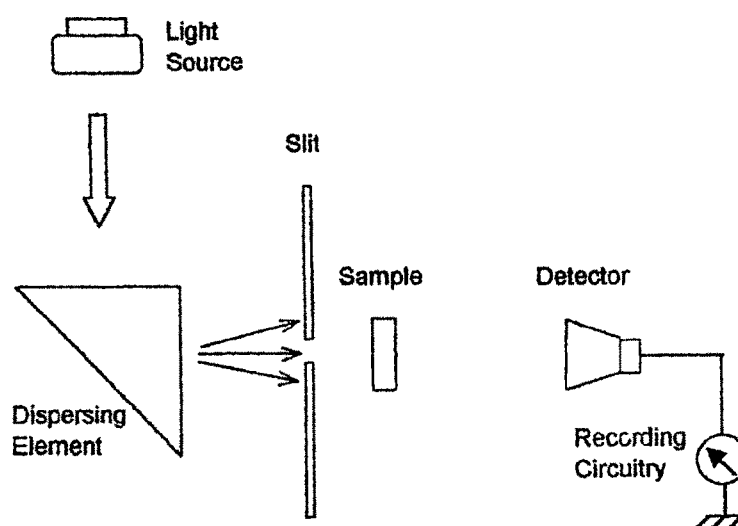


Figure 2.4 Schematic diagram of an optical absorption experiment.

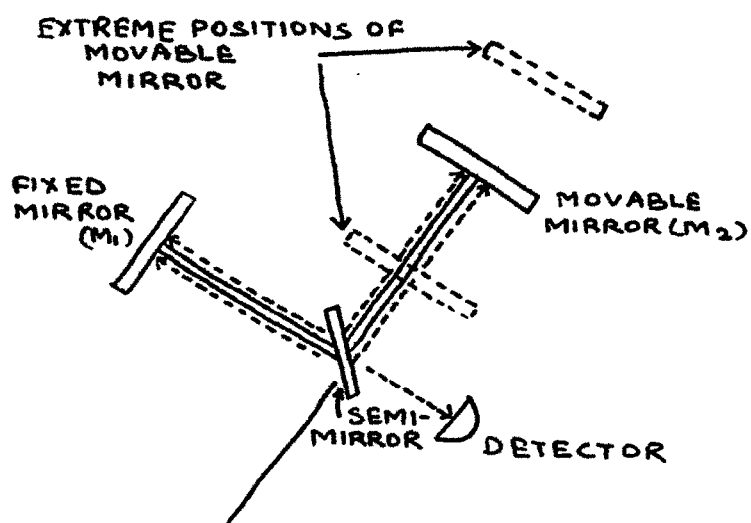


Figure 2.5 The basic components of an interferometer.

Broad band infrared radiation is generated in a source and dispersed by a dispersing element (usually a grating or prism). An appropriately located slit selects a narrow band of wavelengths of the dispersed radiation. This band of wavelengths is incident onto the sample, and a detector measures the amount of the radiation that is transmitted through the sample. The wavelength of radiation that is passed through the slit can be controlled by rotating the dispersing element, so the detector will measure a spectrum of transmitted radiation as the wavelength passing through the sample is varied over the region of interest. Actual dispersive infrared spectrometers are much more complicated than is apparent from the above discussion. Modern machines are often double beam instruments where the difference between the absorption in two different sample chambers is measured. This makes the elimination of absorption due to atmospheric constituents such as CO₂ automatic. It also allows the measurement of absorption introduced into a sample by some external treatment such as ion bombardment. This is accomplished by placing one or two identical samples in each sample compartment and adjusting the spectrometer to measure no difference in absorption. Then one of the samples can be treated and the absorption measurement repeated to yield the difference in absorption induced by the treatment. There are also differences in the way various double beam spectrometers measure the absorption of radiation; for example, optical null spectrometers and ratio recording spectrometers.

If the intensity of radiation incident on the sample at a given wavelength is I_0 and the intensity detected after passing through the sample is I , then the transmittance (T) of the sample at that wavelength is

$$T = I / I_0 = \exp(-abc) \quad (2.12)$$

Where a is the molar absorptivity, b is the sample thickness and c is the concentration of the absorbing species. The absorbance A is then defined by

$$A = \ln(1/T) = abc \quad (2.13)$$

This expression which linearly relates the absorbance of a sample to the concentration of the absorbing species is known as Beer's law and applies to visible and ultraviolet spectroscopy as well as infrared spectroscopy.

Equations (2.12) and (2.13) define the transmission and the absorbance that may be measured experimentally. Both quantities are used in practice and spectra may be plotted as either transmission versus wavenumber or as absorbance versus wavenumber. Absorbance is considered by some as a more fundamental quantity since it is linearly related to the concentration of the absorbing species. An excellent overview of the use of infrared spectroscopy can be obtained from reference [10].

The energy of the photons in this region of the electromagnetic spectrum is such that absorption processes generally corresponds to excitation of molecular vibrational energy levels rather than the higher energy excitation from one electronic level of an atom to another. Thus the absorption spectrum in the infrared is often used as a fingerprint of the molecular species and is often used for organic identification [11]. In ion bombarded insulators and semiconductors, infrared absorption has been used to identify the vibrational bands of chemical moieties formed by interaction of the implanted ions with the atoms of the substrate material.

In the present investigation we have used FTIR spectrometer of Bomem, Canada, (model MB 104), in Physics Department, MSU, Baroda.

2.3.3 Optical Microscopy

The aim of a microscope is to magnify an object so that details invisible to the naked eye may be observed. A simple microscope produces a magnified image, but it can produce only a limited amount of magnification. In order to observe a large order of magnification a compound microscope is used. In this type of microscope several lenses are used. In the compound microscope the required magnification is achieved in two stages as shown in Figure 2.6.

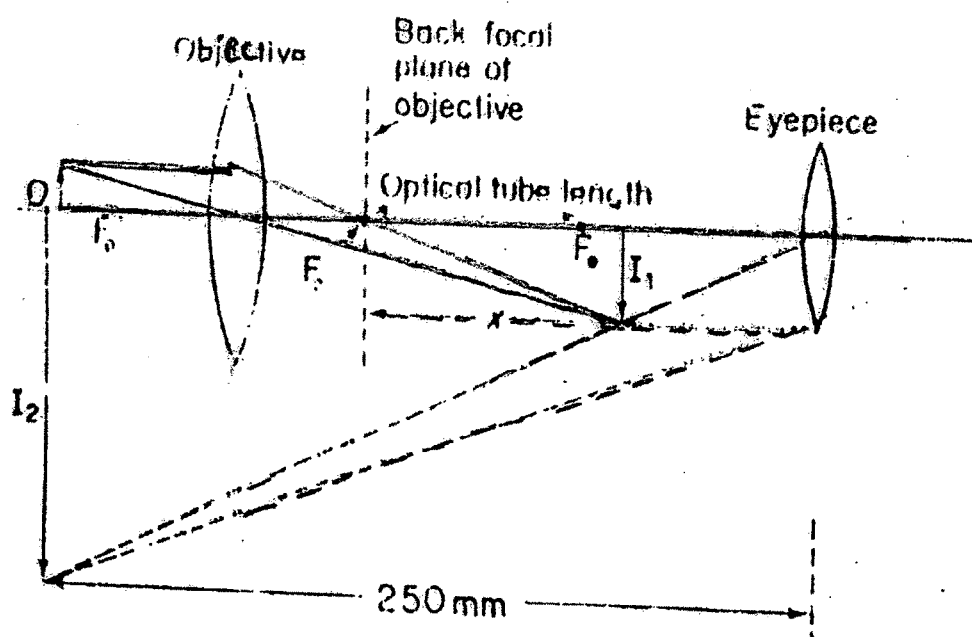


Figure 2.6 Construction of compound microscope.

An objective lens produces an intermediate image I_1 , which is further magnified by the eyepiece thus producing a final virtual image I_2 , which is seen by the observer. The image may be formed at the least distance of distinct vision (conventionally 250 mm), in which case the overall magnification M , of the microscope is given by

$$M = x / f_o [(25 / f_e) + 1] \quad (2.14)$$

In this equation, the expression in brackets represent the magnification due to the eyepiece, which has a focal length f_e , while x/f_o is the magnification produced by the objective, focal length f_o . The distance x is that between the intermediate image and the second focal point of the objective lens. In producing a large overall magnification, the objective usually plays a larger part than the eyepiece. From the above equation it can be seen that a high power objective must have a short focal length, f_o . For example an objective producing an intermediate image ten times as big as the object in a standard microscope has a focal length of 16mm, while for a magnification of forty times the focal length is 4mm.

When large overall magnifications are used or if the microscope is used for long periods, an observer would quickly become tired through eyestrain by observing an image at 250mm. It is much more restful to view the final image at infinity, so that the eye is completely relaxed during observation. This reduces the magnification a little (because of the factor $25 / f_e$ in the above equation), but this disadvantage is more than offset by the reduction in the fatigue suffered by the operator and can be compensated by selecting appropriate combinations of objective and eyepiece to make up the desired magnification. For a particular microscope a range of objective is normally available with magnifications varying from $\times 2$ to $\times 100$ times while eyepieces with a

magnification range of $\times 5$ to $\times 25$ times may be obtained. This means that the maximum overall magnification of the microscope is $\times 2500$ times [13].

For the work of this thesis the microphotographical study of the polymeric surface was carried out using the Vickers projection microscope. It is an inverted metallurgical type optical microscope. This equipment also provides for phase contrast and light profile techniques.

2.3.4 Scanning Electron Microscopy

The interactions of energetic electrons with the surface of a material provide the phenomena that is used for a number of analytical methods, particularly those which analyze near surface regions.

A schematic diagram of a simple scanning electron microscope is shown in **Figure 2.7**. There is a source of electrons, an accelerating electrode, a series of electron lenses to provide a very finely focused spot of electrons on the sample, the specimen, detectors, and the electronics necessary to image the signal of interest. This can be the specimen current, the back-scattered or secondary electrons, or a characteristic X-ray. The electron beam is focused to a fine spot on the sample and the position of the spot on the sample is moved in a pattern called a raster. While the beam is moving, the signal from one of the detectors is displayed on the cathode ray tube, whose beam is also being moved in the same pattern (raster) as the electron beam on the sample. Thus, the picture on the cathode ray tube provides a very magnified image of the signal from the sample [14].

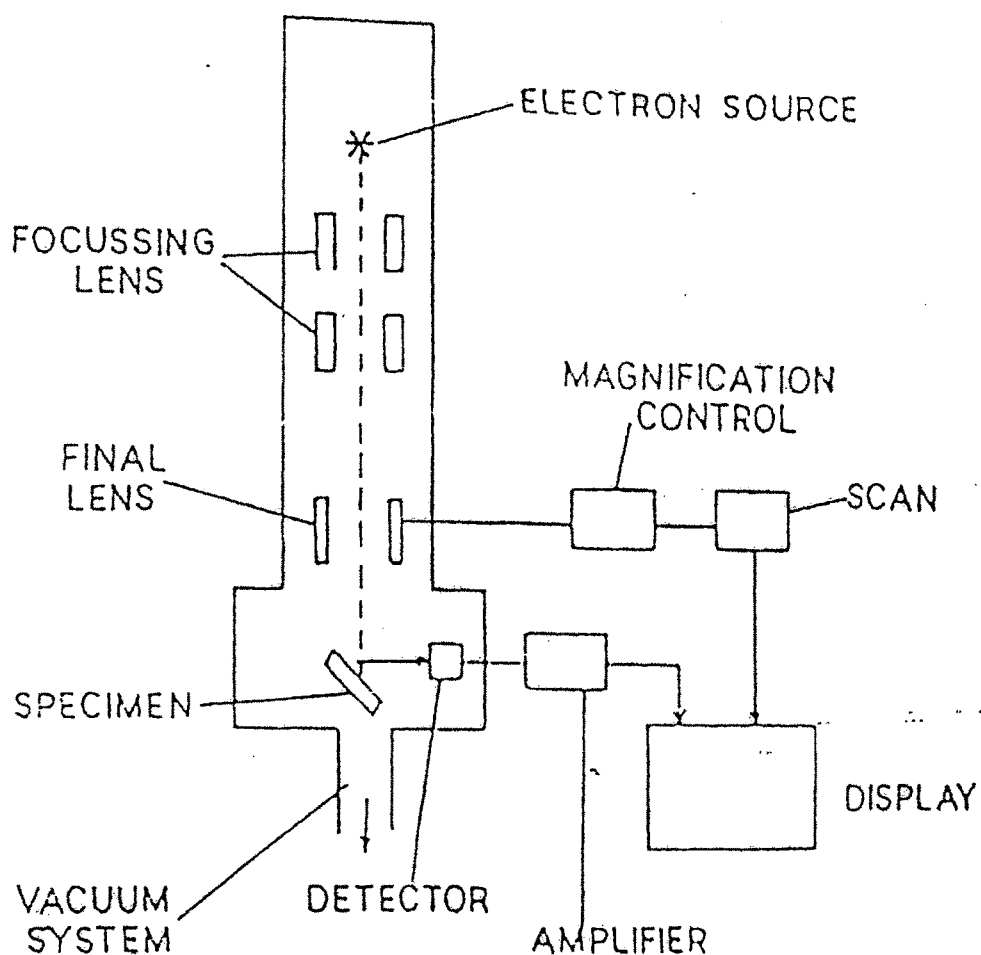


Figure 2.7 Block diagram of a scanning electron microscope

Insulating specimens in electron microscopes tend to charge under exposure to the electron beam. This causes distortion of the image and in many cases a reflection of the incident electrons from the highly charged surface. To overcome this effect, insulating samples are commonly coated with a thin layer of a conducting material to drain away

this surface charge. Carbon is most commonly used for this purpose since it has a low atomic number and causes little interference with the image or with X-ray analysis.

The backscattered and secondary electron images as well as the absorbed current images of a specimen in a scattering electron microscope are sensitive to surface morphology and compositional variations in the near surface region. This is the most common use for scanning electron microscopy on implanted insulators. Additionally, the use of energy dispersive X-ray analysis allows one to map the occurrence of various elemental species across the image area of interest.

SEM is used to get a phenomenological idea of what is happening to the surface of a material when the material is subjected to ion bombardment. The effects of sputtering or ablation or gas bubble formation can be detected. It is not a particularly useful method for quantitative measurements on ion bombarded samples.

The microscope used in our study was Leo, Electron Microscopy, U.K., 440 I, at FCIPT, Gandhinagar.

2.3.5 Vickers' Microhardness Indenter

Hardness of a solid may be broadly defined as its ability to resist penetration by another particular solid. It is a relative property of a material depending on the elastic and plastic properties of both the penetrator and penetrated body. It also depends strongly on the method of testing which combines various material properties like elastic

modulus, yield stress (which is a measure of plastic behaviour or permanent distortion), physical imperfections, impurities and work hardening capacity. Dislocations which constitute the major part of imperfection are usually created by thermal or mechanical stresses at the time of crystal growth or after it. Plastic deformation deliberately introduces new dislocations or moves the ones already present in the crystal. Thus the deformation study may well be effectively used to assess the behaviour of dislocations pertinent to a particular crystal together with the mechanisms of plastic deformation. Plastic deformation study has also been successful by large, to understand the fracture mechanism, particularly in ductile metals and alloys.

The general definition of indentation hardness which is related to various forms of indenters, is the ratio of applied load to the surface area of indentation. Thus hardness has the dimension of stress. Determination of hardness of a material is normally made using a mechanical test that gives a measure of ease with which the material can be locally deformed. Most hardness testers, produce plastic deformation in materials, and they all are based on microscopic indentations made using appropriate loads. The size of the impression of indentation is related to the applied load and the yield stress of the material [15,16].

The load effect of microhardness is an important phenomenon, which needs to be thoroughly investigated to obtain information relating to the laws governing mechanical properties of materials. Hardness is the ratio of load applied to the surface area of indentation which can be calculated using Vickers diamond pyramid indenter.

Vickers diamond indenter:

The Vickers diamond indenter is in the form of a square based pyramid with semi apex angle = 68° . It was used to measure the microhardness of the polymer samples by producing indentation marks on the surfaces of the samples, under known applied loads, loading time, temperature etc. Its main characteristic is the geometrically similar impressions obtained. The Vickers hardness H_v , was calculated using the formula [17]

$$H_v = \frac{1854 \times P}{d^2} \quad \text{Kg/mm}^2$$

$$= \frac{1854 \times P}{d^2} \times 9.8 \quad \text{MPa} \quad (2.15)$$

Where P = load in mN, [obtained as a product of the load in gram (g) and gravitational acceleration $g=9.8 \text{ ms}^{-1}$], and d is the average diagonal length of indentation mark in microns.

To measure the diagonal of the indentation mark, a micrometer eye piece with the least count of 0.125 micron was used. The Vickers Microhardness Tester (supplied by M/s Cooke Toughton and Simms Ltd, England), Photomicrography, (1956) 146 MY (England) was used with the Vickers projection microscope. at Physice Department, MSU, Baroda.

2.3.6 Instron Tensile Tester

The Instron is an American tester which uses the bonded-wire type of strain gauge. In order to accommodate a wide variety of specimens several interchangeable load cells containing the strain gauges are used. In this way a range from 2 to 100,000 g is

possible. The load cell is located centrally in the fixed crosshead. The upper jaw is suspended from the cell through a universal coupling. The lower jaw is mounted on the traversing crosshead which is driven upwards and downwards by screwed rods on each side. A range of gear changes enables the speed of the crosshead, i.e. the rate of extension of the specimen, to be varied in steps from 0.02 to 50 in./min. On the bottom panel of the crosshead assembly the controls which govern the movement of the crosshead can be seen.

The load cell output is fed by cable to the control cabinet which houses the various electronic circuits and the pen recording equipment. The main controls for load range selection, calibration, etc., are mounted on the front panel below the recording chart.

The terminology used is defined as follows.

Load

The application of a load to a specimen in its axial direction causes tension to be developed in the specimen. The 'load' is usually expressed in grams weight or pound weight like gravitational units of force. Where great precision is demanded (e.g. for comparative tests in different parts of the world) the loads measured must be corrected by multiplying by the local value of g , and dividing by 981cm/sec^2 , the standard value).

Breaking load

This is the load at which the specimen breaks, usually expressed in grams weight or pounds weight.

Stress

It is defined as the ratio of the force applied and the cross-sectional area of the specimen.

$$\text{Stress} = \frac{\text{Force Applied}}{\text{Cross-sectional area}}$$

The force is expressed in dynes or poundals.

Breaking Length

The 'breaking length' is the length of the specimen which will just break under its own weight when hung vertically.

Breaking extension.

The 'breaking extension' is the extension of the specimen at the breaking point.

The load weighing system.

The load cell contains a metal beam in the form of a cantilever. Strain gauges, consisting of a grid of very fine wire, are bounded to the surface of the beam. Four strain gauges are used and are connected on the form of a wheatstone bridge each gauge having a nominal resistance of 120Ω . The block circuit diagram is as shown in **Figure**

2.8

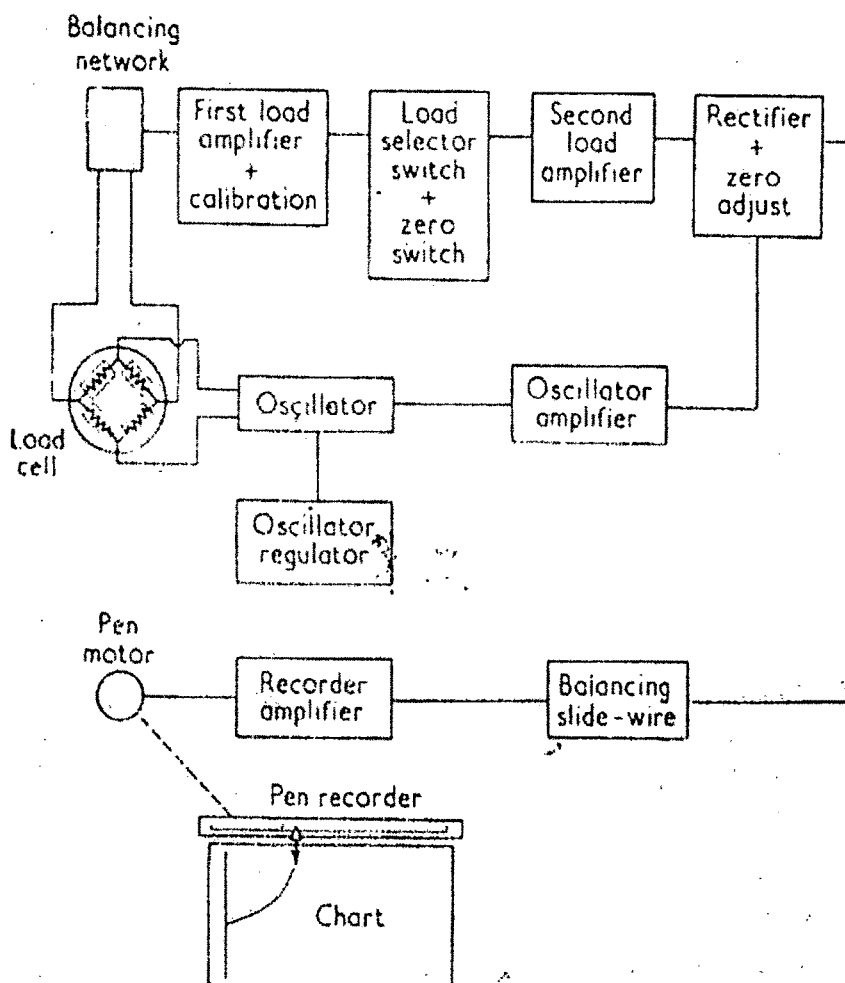


Figure 2.8 Block diagram of Instron Tensile Tester.

Figure 2.8 shows a simplified picture of the method of converting the unbalancing of the bridge into a record of the behaviour of the specimen under load.

The wheatstone bridge network of strain gauges in the load cell is excited from an oscillator at a frequency of 375 c/s. The amplitude of the oscillator is stabilized at a constant value by a separate circuit. An applied load on the cell changes the resistance balance of the bridge and the resulting signal is amplified by a circuit which also includes means for initially balancing the bridge.

The gain of the amplifier can be varied in steps by a load selector switch, and a calibration control can also vary the sensitivity continuously between any of these steps. A zero button shorts out the input to the following amplifier so that the zero position of the recorder may be adjusted without the presence of any load cell signals.

The signal is further amplified and then rectified by a circuit which includes the zero adjustment for the recorder.

From this last circuit the output is a d.c. signal which is fed to the potentiometer type of recorder, where it is compared electrically with the voltage across a balancing slidewire. Any unbalance between the two voltages is converted by a vibrator into a 60 c/s a.c. signal and amplified to operate the pen drive motor, which simultaneously moves the pen and also the slidewire shaft until the recorder is again in balance.

Hence the effect of extending the specimen is to cause the pen to move across the chart a distance proportional to the tensile force in the specimen. If the chart were stationary a straight line whose length represented the size of the load would be drawn, but by moving the chart simultaneously a load-elongation curve is traced by the pen [18].

The instron is a versatile instrument which even in standard form can be used for many types of tests. Various accessories are available which extend the scope of this tester. A selection of the type of tests possible are outlined briefly:

- (1) Load-elongation from zero load to breaking point.
- (2) Elastic recovery from various loads and percentage elongations above and below the yield point.

- (3) Performance of different types of knots in filament yarns.
- (4) Load cycling i.e. repeated loading and unloading between chosen limits.
- (5) Extension cycling.
- (6) Maintenance of a constant load, the creep being taken up automatically.
- (7) Relaxation, measurement of the decay in tension when the specimen is maintained at a constant extension.
- (8) Tearing tests on fabrics.
- (9) Adhesion tests, the measurement of the force required to separate surfaces glued together.
- (10) Compression tests.

Access to this instrument was available at Textile Engineering Department, Faculty of Technology and Engineering, MSU, Baroda, for this work.

2.3.7 Thermogravimetry Analysis

Thermogravimetric analysis is based on the principle of measurement of weight change associated with a transition occurring due to rupture and/or formation of various physical and chemical bonds at elevated temperatures leading to the evolution of volatile products or formation of heavier reaction products.

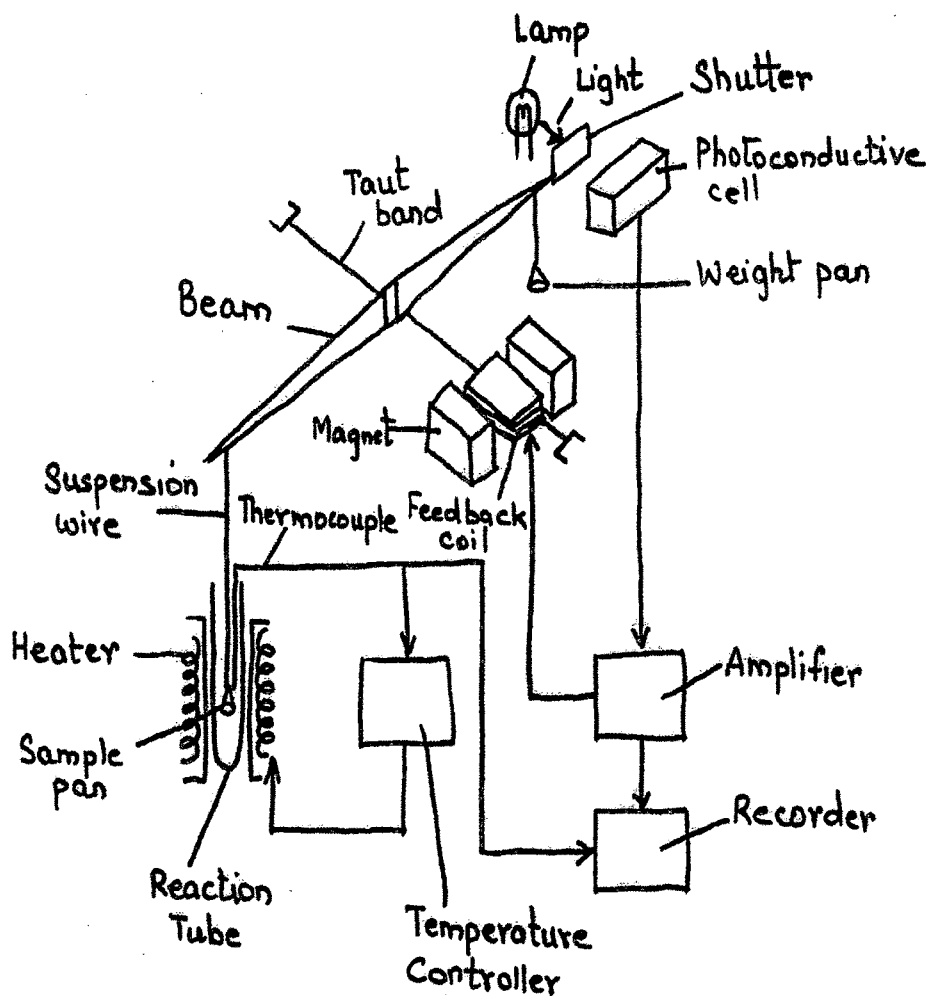


Figure 2.9 Diagram showing principle of TGA.

TGA consists of a sensitive balance and a well-controlled furnace or other suitable heating system to maintain a specified temperature as shown in Figure 2.9. Data collected during a TGA experiment includes time, temperature and sample weight. The sample is placed in a platinum cell, which is then put on the sample pan, suspended in a

quartz or alumina reaction tube, the atmosphere of which can be controlled. In the meantime, weights are placed on the weight pan to approximately balance the sample.

When the weight of the sample changes upon heating, the beam held by the taut band inclines. This inclination is detected by the photoconductive cell, and amplified. A current is allowed to flow through the feedback coil, placed in a uniform magnetic field, to produce a torque (electromagnetic force) to keep the beam horizontal. This is called the null method. Since the torque varies in proportion to the current, the change of sample weight can be exactly measured by recording the current [12].

- TGA is often used for studying degradation. Two aspects of degradation that are studied are thermal degradation and oxidative degradation of polymers. Thermal degradation is important because degradation that occurs during processing (such as extrusion) may be largely thermal and not oxidative. Polymers often degrade by the elimination of a hydrohalogen molecule, so the weight loss is directly related to the rate of polymer degradation. Oxidative degradation is also studied by TGA. In this study, the weight loss profile is different from that for thermal degradation studies, but is more applicable to performance at high temperatures.
- TGA is also used in quality control applications to verify that a given lot of material is the same as a control sample of that chemical. The degradation of polymers can be important for determining the maximum temperature up to which a polymer system can be used. When a polymer chain breaks, some exothermic energy is related with the process. Measuring the energy release gives a measure

of the extent of degradation. In addition to being used to study the oxidative degradation of polymers, calorimetry is used to study the oxidation of polymers without additives.

In this work TGA was performed on Shimadzu Thermogravimetry system TGA-30, at ERDA, Makarpura, Baroda and SIEKO thermal analyzer TGA-220 at ABS-Bayer, Moxi, India.

REFERENCES

- (1) D. Kanjilal, S. Chopra, M.M. Narayanan, I.S. Iyer, V. Jha, R. Joshi, S.K.Datta, Nuclear Instr. And Method. A 238 (1993) 97. G.K. Mehta, A.P. Patro, Nucl. Inst. And Meth.A268 (1988) 334.
- (2) Proceedings of, Ion Beam Modification of Insulators edited by P. Mazzoldi and G. W. Arnold, Elsevier Science, Amsterdam, 1987.
- (3) Dole and Malcolm, The radiation chemistry of macromolecules, Academic press, Volume I (1972), Volume II (1973)
- (4) Chopra, K.L. Thin Films Phenomena. New York, McGraw-Hill, 1969.
- (5) Handbook of Materials Science. Ed. C.T. Lynch. Vol. 1-3. Cleveland, CRS Press, 1974-1975.
- (6) T. Murayama, Dynamic Mechanical Analysis of Polymeric Material, Elsevier, Amsterdam, 1978.
- (7) J.K. Gillham, in developments in Polymer Characterisation-3, J.V. Dawkins, ed., Applied Science Publishers, Ltd., London, 1982,159.
- (8) J. R. Fried, A. Letton, and W.J. welsh, Polymer, 31, (1990) 1032.
- (9) K. Walters, Rheometry, Chapman and Hall, London, 1975.
- (10) A. Lee Smith, Applied Infrared spectroscopy, Chemical Analysis, Vol. 54, John Wiley & Sons, New York, 1979.
- (11) L.J. Bellamy, The Infra-red Spectra of Complex Molecules, Vol. 1., 3rd edn., Chapman and Hall, London, 1975.
- (12) L.C. Martin, The theory of the Microscope. Blackie, London, (1966).